
RAIL: Risk-Averse Imitation Learning

Anirban Santara*
IIT Kharagpur
anirban_santara@iitkgp.ac.in

Abhishek Naik* **Balaraman Ravindran**
IIT Madras
{anaik, ravi}@cse.iitm.ac.in

Dipankar Das **Dheevatsa Mudigere** **Sasikanth Avancha** **Bharat Kaul**
Parallel Computing Lab - Intel Labs, India
{dipankar.das, dheevatsa.mudigere, sasikanth.avancha, bharat.kaul}@intel.com

Abstract

Imitation learning algorithms learn viable policies by imitating an expert’s behavior when reward signals are not available. Generative Adversarial Imitation Learning (GAIL) is a state-of-the-art algorithm for learning policies when the expert’s behavior is available as a fixed set of trajectories. We evaluate in terms of the expert’s cost function and observe that the distribution of trajectory-costs is often more heavy-tailed for GAIL-agents than the expert at a number of benchmark continuous-control tasks. Thus, high-cost trajectories, corresponding to tail-end events of catastrophic failure, are more likely to be encountered by the GAIL-agents than the expert. This makes the reliability of GAIL-agents questionable when it comes to deployment in risk-sensitive applications like robotic surgery and autonomous driving. In this work, we aim to minimize the occurrence of tail-end events by minimizing tail risk within the GAIL framework. We quantify tail risk by the Conditional-Value-at-Risk (*CVaR*) of trajectories and develop the Risk-Averse Imitation Learning (RAIL) algorithm. We observe that the policies learned with RAIL show lower tail-end risk than those of vanilla GAIL. Thus the proposed RAIL algorithm appears as a potent alternative to GAIL for improved reliability in risk-sensitive applications.

1 Introduction

Reinforcement learning (RL) [Sutton and Barto, 1998] is used to learn an effective policy of choosing actions in order to achieve a specified goal in an environment. The goal is communicated to the agent through a scalar cost and the agent learns a policy that minimizes the expected total cost incurred over a trajectory. RL algorithms, along with efficient function approximators like deep neural networks, have achieved human-level or beyond human-level performance at many challenging planning tasks like continuous-control [Lillicrap et al., 2015, Schulman et al., 2015] and game-playing [Silver et al., 2016, Mnih et al., 2015]. In classical RL, the cost function is handcrafted based on heuristic assumptions about the goal and the environment. This is challenging in most real-world applications and also prone to subjectivity induced bias. Imitation learning or Learning from Demonstration (LfD) [Argall et al., 2009, Schaal, 1997, Atkeson and Schaal, 1997, Abbeel and Ng, 2011, 2004, Ng et al., 2000] addresses this challenge by providing methods of learning policies through imitation of an expert’s behavior without the need of a handcrafted cost function. In this paper we study the reliability of existing imitation learning algorithms when it comes to learning solely from a fixed set of trajectories demonstrated by an expert with no interaction between the agent and the expert during training.

*Authors contributed equally as a part of their internship at Parallel Computing Lab - Intel Labs, India.

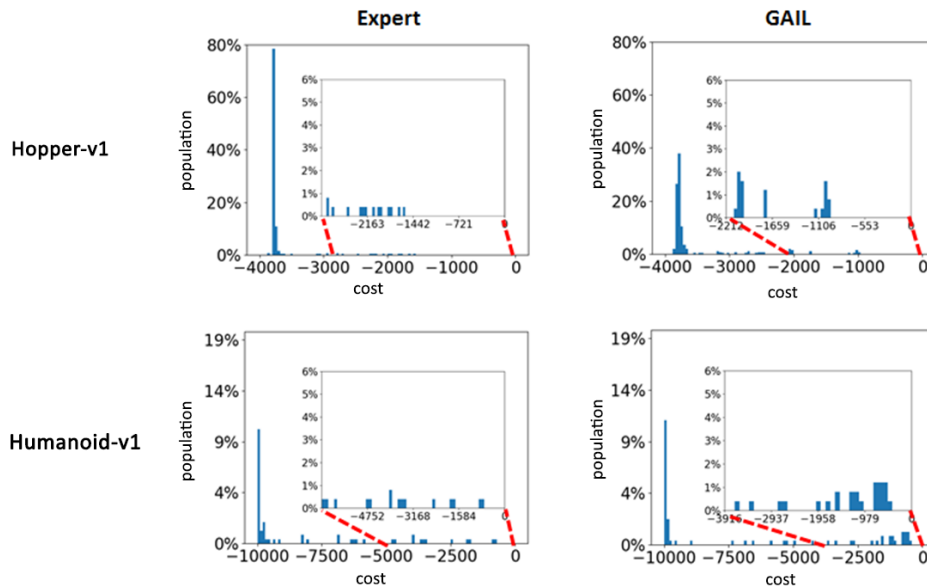


Figure 1: Histograms of the costs of 250 trajectories generated by the expert and GAIL agents at high-dimensional continuous control tasks, Hopper-v1 and Humanoid-v1, from OpenAI Gym. The inset diagrams show zoomed-in views of the tails of these distributions (the region beyond 2σ of the mean). We observe that the GAIL agents produce tails heavier than the expert, indicating that GAIL is more prone to generating high-cost trajectories.

Imitation learning algorithms fall into two broad categories. The first category, known as Behavioral Cloning [Pomerleau, 1989, Bojarski et al., 2016, 2017], uses supervised learning to fit a policy function to the state-action pairs from expert-demonstrated trajectories. Despite its simplicity, Behavioral Cloning fails to work well when only a limited amount of data is available. These algorithms assume that observations are i.i.d. and learn to fit single time-step decisions. Whereas, in sequential decision making problems where predicted actions affect the future observations (e.g. driving), the i.i.d. assumption is violated. As a result, these algorithms suffer from the problem of compounding error due to covariate shift [Ross and Bagnell, 2010, Ross et al., 2011]. Approaches to ameliorate the issue of compounding error like SMILe [Ross and Bagnell, 2010], SEARN [Daumé et al., 2009], CPI [Kakade and Langford, 2002] suffer from instability in practical applications [Ross et al., 2011] while DAGGER [Ross et al., 2011] and AGGREGATE [Ross and Bagnell, 2014] require the agent to query the expert during training which is not allowed in our setting of learning from a fixed set of expert demonstrations. Another drawback of Behavioral Cloning is that it does not allow the agent to explore alternate policies for achieving the same objective that might be efficient in some sense other than what the expert cared for.

The second category of algorithms is known as Inverse Reinforcement Learning (IRL) (Russell [1998], Ng et al. [2000], Abbeel and Ng [2011]). It attempts to uncover the underlying reward function that the expert is trying to maximize from a set of expert-demonstrated trajectories. This reward function succinctly encodes the expert’s behavior and can be used by an agent to learn a policy through an RL algorithm. The method of learning policies through RL after IRL is known as Apprenticeship Learning (Abbeel and Ng [2004]). IRL algorithms find reward functions that prioritize entire trajectories over others. Unlike behavioral cloning, they do not fit single time-step decisions, and hence they do not suffer from the issue of compounding error. However, IRL algorithms are indirect because they learn a reward function that explains expert behavior but do not tell the learner how to act directly (Ho and Ermon [2016]). The job of learning an actionable policy is left to RL algorithms. Moreover, IRL algorithms are computationally expensive and have scalability issues in large environments (Finn et al. [2016], Levine and Koltun [2012]).

The recently proposed Generative Adversarial Imitation Learning (GAIL) algorithm [Ho and Ermon, 2016] presents a novel mathematical framework in which the agent learns to act by directly extracting a policy from expert-demonstrated trajectories, as if it were obtained by RL following IRL. The authors show that unlike Behavioral Cloning, this method is not prone to the issue of compounding error and it is also scalable to large environments. Currently, GAIL provides state-of-the-art performance at several benchmark control tasks, including those in Table 1.

Risk sensitivity is integral to human learning [Nagengast et al., 2010, Niv et al., 2012], and risk-sensitive decision-making problems, in the context of MDPs, have been investigated in various fields, e.g., in finance [Ruszczyński, 2010], operations research [Howard and Matheson, 1972, Borkar, 2002], machine learning [Heger, 1994, Mihatsch and Neuneier, 2002] and robotics [Shalev-Shwartz et al., 2016, 2017, Abbeel et al., 2007, Rajeswaran et al., 2016]. [Garcia and Fernández, 2015] give a comprehensive overview of different risk-sensitive RL algorithms. They fall in two broad categories. The first category includes methods that constrain the agent to safe states during exploration while the second modifies the optimality criterion of the agent to embed a term for minimizing risk. Studies on risk-minimization are rather scarce in the imitation learning literature. [Majumdar et al., 2017] take inspiration from studies like [Glimcher and Fehr, 2013, Shen et al., 2014, Hsu et al., 2005] on modeling risk in human decision-making and conservatively approximate the expert’s risk preferences by finding an outer approximation of the risk envelope. Much of the literature on imitation learning has been developed with average-case performance at the center, overlooking tail-end events. In this work, we aim to take an inclusive and direct approach to minimizing tail risk of GAIL-learned policies at test time irrespective of the expert’s risk preferences.

In order to evaluate the worst-case risk of deploying GAIL-learned policies, we studied the distributions (see Figure 1) of trajectory-costs (according to the expert’s cost function) for the GAIL agents and experts at different control tasks (see Table 1). We observed that the distributions for GAIL are more heavy-tailed than the expert, where the tail corresponds to occurrences of high trajectory-costs. In order to quantify tail risk, we use Conditional-Value-at-Risk ($CVaR$) [Rockafellar and Uryasev, 2000]. $CVaR$ is defined as the expected cost above a given level of confidence and is a popular and coherent tail risk measure. The heavier the tail, the higher the value of $CVaR$. We observe that the value of $CVaR$ is much higher for GAIL than the experts at most of the tasks (see Table 1) which again suggests that the GAIL agents encounter high-cost trajectories more often than the experts. Since high trajectory-costs may correspond to events of catastrophic failure, GAIL agents are not reliable in risk-sensitive applications. In this work, we aim to explicitly minimize expected worst-case risk for a given confidence bound (quantified by $CVaR$) along with the GAIL objective, such that the learned policies are more reliable than GAIL, when deployed, while still preserving the average performance of GAIL. [Chow and Ghavamzadeh, 2014] developed policy gradient and actor-critic algorithms for mean- $CVaR$ optimization for learning policies in the classic RL setting. However these algorithms are not directly applicable in our setting of learning a policy from a set of expert-demonstrated trajectories. We take inspiration from this work and make the following contributions:

1. We formulate the Risk-Averse Imitation Learning (RAIL) algorithm which optimizes $CVaR$ in addition to the original GAIL objective.
2. We evaluate RAIL at a number of benchmark control tasks and demonstrate that it obtains policies with lesser tail risk at test time than GAIL.

The rest of the paper is organized as follows. Section 2 builds the mathematical foundation of the paper by introducing essential concepts of imitation learning. Section 3 defines relevant risk-measures and describes the proposed Risk-Averse Imitation Learning algorithm. Section 4 specifies our experimental setup and Section 5 outlines the evaluation metrics. Finally, Section 6 presents the results of our experiments comparing RAIL with GAIL followed by a discussion of the same and Section 7 concludes the paper with scope of future work.

2 Mathematical Background

Let us consider a Markov Decision Process (MDP), $\mathcal{M} = (\mathcal{S}, \mathcal{A}, \mathcal{T}, c, p_0, \gamma)$, where \mathcal{S} denotes the set of all possible states, \mathcal{A} denotes the set of all possible actions that the agent can take, $\mathcal{T} : \mathcal{S} \times \mathcal{A} \times \mathcal{S} \rightarrow [0, 1]$ is the state transition function such that, $T(s'|s, a)$ is a probability distribution over next states, $s' \in \mathcal{S}$ given current state $s \in \mathcal{S}$ and action $a \in \mathcal{A}$, $c : \mathcal{S} \times \mathcal{A} \rightarrow \mathbb{R}$ is the cost function which generates a real number as feedback for every state-action pair, $p_0 : \mathcal{S} \rightarrow [0, 1]$ gives the initial state distribution, and γ is a temporal discount factor.

A policy $\pi : \mathcal{S} \times \mathcal{A} \rightarrow [0, 1]$ is a function such that $\pi(a|s)$ gives a probability distribution over actions, $a \in \mathcal{A}$ in a given state, $s \in \mathcal{S}$. Let $\xi = (s_0, a_0, s_1, \dots, s_{L_\xi})$ denote a trajectory of length L_ξ , obtained by following a policy π . We define expectation of a function $f(\cdot, \cdot)$ defined on $\mathcal{S} \times \mathcal{A}$ with respect to a policy π as follows:

$$\mathbb{E}_\pi[f(s, a)] \triangleq \mathbb{E}_{\xi \sim \pi} \left[\sum_{t=0}^{L_\xi-1} \gamma^t f(s_t, a_t) \right] \quad (1)$$

2.1 Generative Adversarial Imitation Learning

Apprenticeship learning or Apprenticeship Learning via Inverse Reinforcement Learning algorithms [Abbeel and Ng, 2004] first estimate the expert’s reward function using IRL and then find the optimal policy for the recovered reward function using RL. Mathematically, this problem can be described as:

$$RL \circ IRL(\pi_E) = \underset{\pi \in \Pi}{\operatorname{argmin}} \max_{c \in \mathcal{C}} \mathbb{E}_\pi[c(s, a)] - \mathbb{E}_{\pi_E}[c(s, a)] - H(\pi) \quad (2)$$

where, π_E denotes the expert-policy. $c(\cdot, \cdot)$ denotes the cost function. Π and \mathcal{C} denote the hypothesis classes for policy and cost functions. $H(\pi)$ denotes entropy of policy π . The term $-H(\pi)$ provides causal-entropy regularization [Ziebart, 2010, Ziebart et al., 2008] which helps in making the policy optimization algorithm unbiased to factors other than the expected reward.

[Ho and Ermon, 2016] proposed Generative Adversarial Imitation Learning (GAIL) which packs the two step process of $RL \circ IRL_\psi(\pi_E)$ into a single optimization problem with special considerations for scalability in large environments. The name is due to the fact that this objective function can be optimized using the Generative Adversarial Network (GAN) [Goodfellow et al., 2014] framework. The following is objective function of GAIL:

$$\underset{\pi \in \Pi}{\operatorname{argmin}} \max_{\mathcal{D} \in (0,1)^{\mathcal{S} \times \mathcal{A}}} \mathbb{E}_\pi[\log(\mathcal{D}(s, a))] + \mathbb{E}_{\pi_E}[\log(1 - \mathcal{D}(s, a))] - H(\pi) \quad (3)$$

Here, the agent’s policy, π , acts as a *generator* of state-action pairs. \mathcal{D} is a discriminative binary classifier of the form $\mathcal{D} : \mathcal{S} \times \mathcal{A} \rightarrow (0, 1)$, known as *discriminator*, which given a state-action pair (s, a) , predicts the likelihood of it being generated by the generator. A two-player adversarial game is started, wherein the generator tries to generate (s, a) pairs that closely match the expert, while the discriminator tries to correctly classify the (s, a) pairs of the expert and the agent. At convergence, the agent’s actions resemble those of the expert in any given state.

The generator and the discriminator are assigned parameterized models π_θ and \mathcal{D}_w respectively. The training algorithm alternates between a *gradient ascent* step with respect to the discriminator parameters, w , and a *policy-gradient descent* step with respect to the generator parameters, θ . Following the example of [Ho and Ermon, 2016] we use multi-layer perceptrons (neural networks with fully-connected layers) [Haykin, 1998] to model both the generator and the discriminator.

3 Risk-Averse Imitation Learning

In this section, we develop the mathematical formulation of the proposed Risk-Averse Imitation Learning (RAIL) algorithm. We introduce *CVaR* [Rockafellar and Uryasev, 2000] as a measure of tail risk, and apply it in the GAIL-framework to minimize the tail risk of learned policies.

3.1 Conditional-Value-at-Risk

In the portfolio-risk optimization literature, tail risk is a form of portfolio risk that arises when the possibility that an investment moving more than three standard deviations away from the mean is greater than what is shown by a normal distribution [Investopedia, 2017]. Tail risk corresponds to events that have a small probability of occurring. When the distribution of market returns is heavy-tailed, tail risk is high because there is a probability, which may be small, that an investment will move beyond three standard deviations.

Conditional-Value-at-Risk (*CVaR*) [Rockafellar and Uryasev, 2000] is the most conservative measure of tail risk [Dalleh, 2011]. Unlike other measures like Variance and Value at Risk (*VaR*), it can

be applied when the distribution of returns is not normal. Mathematically, let Z be a random variable. Let $\alpha \in [0, 1]$ denote a probability value. The *Value-at-Risk* of Z with respect to confidence level α , denoted by $VaR_\alpha(Z)$, is defined as the minimum value $z \in \mathbb{R}$ such that with probability α , Z will not exceed z .

$$VaR_\alpha(Z) = \min(z \mid P(Z \leq z) \geq \alpha) \quad (4)$$

$CVaR_\alpha(Z)$ is defined as the conditional expectation of losses above $VaR_\alpha(Z)$:

$$CVaR_\alpha(Z) = \mathbb{E}[Z \mid Z \geq VaR_\alpha(Z)] = \min_{\nu \in \mathbb{R}} H_\alpha(Z, \nu) \quad (5)$$

where $H_\alpha(Z, \nu)$ is given by:

$$H_\alpha(Z, \nu) \triangleq \left\{ \nu + \frac{1}{1-\alpha} \mathbb{E}[(Z - \nu)^+] \right\}; \quad (x)^+ = \max(x, 0) \quad (6)$$

3.2 RAIL Framework

We use $CVaR$ to quantify the tail risk of the trajectory-cost variable $\mathcal{R}^\pi(\xi|c(\mathcal{D}))$, defined in the context of GAIL as:

$$\mathcal{R}^\pi(\xi|c(\mathcal{D})) = \sum_{t=0}^{L_\xi-1} \gamma^t c(\mathcal{D}(s_t, a_t)) \quad (7)$$

where $c(\cdot)$ is order-preserving.

Next, we formulate the optimization problem to optimize $CVaR$ of $\mathcal{R}^\pi(\xi|c(\mathcal{D}))$ as:

$$\min_{\pi} \max_c CVaR_\alpha(\mathcal{R}^\pi(\xi|c(\mathcal{D}))) = \min_{\pi, \nu} \max_c H_\alpha(\mathcal{R}^\pi(\xi|c(\mathcal{D})), \nu) \quad (8)$$

Integrating this with the GAIL objective of equation 3, we have the following:

$$\begin{aligned} \min_{\pi, \nu} \max_{\mathcal{D} \in (0,1)^{\mathcal{S} \times \mathcal{A}}} \mathcal{J} = \min_{\pi, \nu} \max_{\mathcal{D} \in (0,1)^{\mathcal{S} \times \mathcal{A}}} \left\{ -H(\pi) + \mathbb{E}_\pi[\log(\mathcal{D}(s, a))] \right. \\ \left. + \mathbb{E}_{\pi_E}[\log(1 - \mathcal{D}(s, a))] + \lambda_{CVaR} H_\alpha(\mathcal{R}^\pi(\xi|c(\mathcal{D})), \nu) \right\} \quad (9) \end{aligned}$$

Note that as $c(\cdot)$ is order-preserving, the maximization with respect to c in equation 8 is equivalent to maximization with respect to \mathcal{D} in equation 9. λ_{CVaR} is a constant that controls the amount of weightage given to $CVaR$ optimization relative to the original GAIL objective. Equation 9 comprises the objective function of the proposed Risk-Averse Imitation Learning (RAIL) algorithm. Algorithm 1 gives the pseudo-code. Appendix A derives the expressions of gradients of the $CVaR$ term $H_\alpha(\mathcal{R}^\pi(\xi|c(\mathcal{D})), \nu)$ with respect to π , \mathcal{D} , and ν . When $\alpha \rightarrow 0$, namely the risk-neutral case, $CVaR$ is equal to the mean of all trajectory costs and hence, RAIL \rightarrow GAIL. We use Adam algorithm [Diederik Kingma, 2015] for gradient ascent in the discriminator and Trust Region Policy Optimization (TRPO) [Schulman et al., 2015] for policy gradient descent in the generator. The $CVaR$ term ν is trained by batch gradient descent [Haykin, 1998].

4 Experimental Setup

We compare the tail risk of policies learned by GAIL and RAIL for five continuous control tasks listed in Table 1. All these environments, were simulated using MuJoCo Physics Simulator [Todorov et al., 2012]. Each of these environments come packed with a “true” reward function in OpenAI Gym [Brockman et al., 2016]. [Ho and Ermon, 2016] trained neural network policies using Trust Region Policy Optimization (TRPO) [Schulman et al., 2015] on these reward functions to achieve state-of-the-art performance and have made the pre-trained models publicly available for all these environments as a part of their repository [OpenAI-GAIL, 2017]. They used these policies to generate the expert trajectories in their work on GAIL [Ho and Ermon, 2016]. For a fair comparison, we use the same policies to generate expert trajectories in our experiments. Table 1 gives the number of expert trajectories sampled for each environment. These numbers correspond to the best results reported in [Ho and Ermon, 2016].

Algorithm 1 Risk-Averse Imitation learning (RAIL)

Input: Expert trajectories $\xi_E \sim \pi_E$, hyper-parameters $\alpha, \beta, \lambda_{CVaR}$ **Output:** Optimized learner’s policy π

- 1: Initialization: $\theta \leftarrow \theta_0, w \leftarrow w_0, \nu \leftarrow \nu_0, \lambda \leftarrow \lambda_{CVaR}$
 - 2: **repeat**
 - 3: Sample trajectories $\xi_i \sim \pi_{\theta_i}$
 - 4: Estimate $\hat{H}_\alpha(D^\pi(\xi|c(\mathcal{D})), \nu) = \nu + \frac{1}{1-\alpha} \mathbb{E}_{\xi_i} [(D^\pi(\xi|c(\mathcal{D})) - \nu)^+]$
 - 5: Gradient ascent on discriminator parameters using:

$$\nabla_{w_i} \mathcal{J} = \hat{\mathbb{E}}_{\xi_i} [\nabla_{w_i} \log(\mathcal{D}(s, a))] + \hat{\mathbb{E}}_{\xi_E} [\nabla_{w_i} \log(1 - \mathcal{D}(s, a))] + \lambda_{CVaR} \nabla_{w_i} H_\alpha(\mathcal{R}^\pi(\xi|c(\mathcal{D})), \nu)$$
 - 6: KL-constrained natural gradient descent step (TRPO) on policy parameters using:

$$\nabla_{\theta_i} \mathcal{J} = \mathbb{E}_{(s,a) \sim \xi_i} [\nabla_{\theta_i} \log \pi_\theta(a|s) Q(s, a)] - \nabla_{\theta_i} H(\pi_\theta) + \lambda_{CVaR} \nabla_{\theta_i} H_\alpha(\mathcal{R}^\pi(\xi|c(\mathcal{D})), \nu)$$
 where $Q(\bar{s}, \bar{a}) = \mathbb{E}_{(s,a) \sim \xi_i} [\log(\mathcal{D}_{w_{i+1}}(s, a)) | s_0 = \bar{s}, a_0 = \bar{a}]$
 - 7: Gradient descent on CVaR parameters:

$$\nabla_{\nu_i} \mathcal{J} = \nabla_{\nu_i} H_\alpha(\mathcal{R}^\pi(\xi|c(\mathcal{D})), \nu)$$
 - 8: **until** $i == \text{max_iter}$
-

Again, following [Ho and Ermon, 2016], we model the generator (policy), discriminator and value function (used for advantage estimation [Sutton and Barto, 1998] for the generator) with multi-layer perceptrons of the following architecture: `observationDim - fc_100 - tanh - fc_100 - tanh - outDim`, where `fc_100` means fully connected layer with 100 nodes, `tanh` represents the hyperbolic-tangent activation function of the hidden layers, `observationDim` stands for the dimensionality of the observed feature space, `outDim` is equal to 1 for the discriminator and value function networks and equal to the twice of the dimensionality of the action space (for mean and standard deviation of the Gaussian from which the action should be sampled) for the policy network. For example, in case of Humanoid-v1, `observationDim = 376` and `outDim = 34` in the policy network. The value of the CVaR coefficient λ_{CVaR} is set as given by Table 1 after a coarse hyperparameter search. All other hyperparameters corresponding to the GAIL component of the algorithm are set identical to those used in [Ho and Ermon, 2016] and their repository [OpenAI-GAIL, 2017] for all the experiments. The value of α in the CVaR term is set to 0.9 and its lone parameter, ν , is trained by batch gradient descent with learning rate 0.01.

5 Evaluation Metrics

In this section we define the metrics we use to evaluate the efficacy of RAIL at reducing the tail risk of GAIL learned policies. Given an agent A ’s policy π_A we roll out N trajectories $T = \{\xi_i\}_{i=1}^N$ from it and estimate VaR_α and $CVaR_\alpha$ as defined in Section 3.1. VaR_α denotes the value under

Table 1: Hyperparameters for the RAIL experiments on various continuous control tasks from OpenAI Gym. For a fair comparison, the number of training iterations and expert trajectories are same as those used by [Ho and Ermon, 2016].

Task	#training iterations	#expert trajectories	λ_{CVaR}
Reacher-v1	200	18	0.25
HalfCheetah-v1	500	25	0.5
Hopper-v1	500	25	0.5
Walker-v1	500	25	0.25
Humanoid-v1	1500	240	0.75

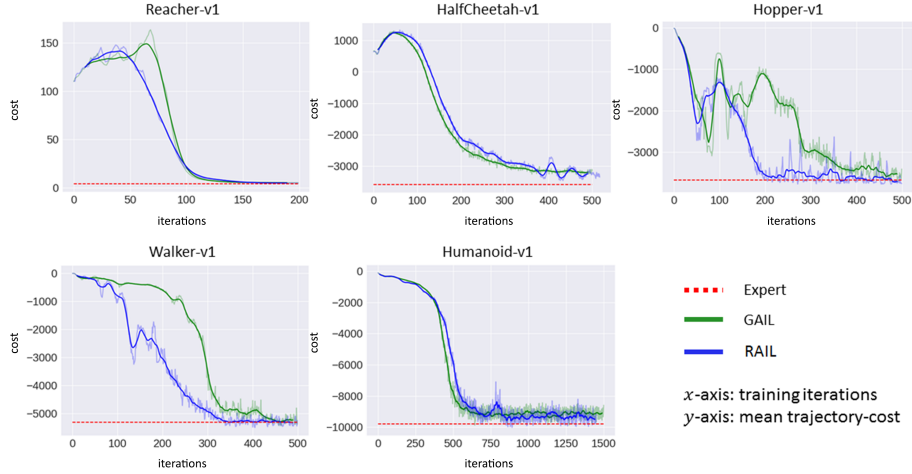


Figure 2: Convergence of mean trajectory-cost during training. The faded curves corresponds to the original value of mean trajectory-cost which varies highly between successive iterations. The data is smoothened with a moving average filter of window size 21 to demonstrate the prevalent behavior and plotted with solid curves. RAIL converges almost as fast as GAIL at all the five continuous-control tasks, and at times, even faster.

which the trajectory-cost remains with probability α and $CVaR_\alpha$ gives the expected value of cost above VaR_α . Intuitively, $CVaR_\alpha$ gives the average value of cost of the worst cases that have a total probability no more than $(1 - \alpha)$. The lower the value of both these metrics, the lower is the tail risk.

In order to compare tail risk of an agent with respect to the expert, E , we define percentage relative- VaR_α as follows:

$$VaR_\alpha(A|E) = 100 \times \frac{VaR_\alpha(E) - VaR_\alpha(A)}{|VaR_\alpha(E)|} \% \quad (10)$$

Similarly, we define percentage relative- $CVaR_\alpha$ as:

$$CVaR_\alpha(A|E) = 100 \times \frac{CVaR_\alpha(E) - CVaR_\alpha(A)}{|CVaR_\alpha(E)|} \% \quad (11)$$

The higher these numbers, the lesser is the tail risk of agent A . We define Gain in Reliability (GR) as the difference in percentage relative tail risk between RAIL and GAIL agents.

$$GR-VaR = VaR_\alpha(RAIL|E) - VaR_\alpha(GAIL|E) \quad (12)$$

$$GR-CVaR = CVaR_\alpha(RAIL|E) - CVaR_\alpha(GAIL|E) \quad (13)$$

Table 2: Comparison of expert, GAIL, and RAIL in terms of the tail risk metrics - $VaR_{0.9}$ and $CVaR_{0.9}$. All the scores are calculated on samples of 50 trajectories. With smaller values of VaR and $CVaR$, our method outperforms GAIL in all the 5 continuous control tasks and also outperforms the expert in many cases.

Environment	Dimensionality		VaR			CVaR		
	Observation	Action	Expert	GAIL	Ours	Expert	GAIL	Ours
Reacher-v1	11	2	5.88	9.55	7.28	6.34	13.25	9.41
Hopper-v1	11	3	-3754.71	-1758.19	-3745.90	-2674.65	-1347.60	-3727.94
HalfCheetah-v1	17	6	-3431.59	-2688.34	-3150.31	-3356.67	-2220.64	-2945.76
Walker-v1	17	6	-5402.52	-5314.05	-5404.00	-2310.54	-3359.29	-3939.99
Humanoid-v1	376	17	-9839.79	-2641.14	-9252.29	-4591.43	-1298.80	-4640.42

Table 3: Values of percentage relative tail risk measures and gains in reliability on using RAIL over GAIL for different continuous control tasks.

Environment	$VaR_{0.9}(A E)(\%)$		GR-VaR (%)	$CVaR_{0.9}(A E)(\%)$		GR-CVaR (%)
	GAIL	RAIL		GAIL	RAIL	
Reacher-v1	-62.41	-23.81	38.61	-108.99	-48.42	60.57
Hopper-v1	-53.17	-0.23	52.94	-49.62	39.38	89.00
HalfCheetah-v1	-21.66	-8.20	13.46	-33.84	-12.24	21.60
Walker-v1	-1.64	0.03	1.66	45.39	70.52	25.13
Humanoid-v1	-73.16	-5.97	67.19	-71.71	1.07	72.78

6 Experimental Results and Discussion

In this section, we present and discuss the results of comparison between GAIL and RAIL. The expert’s performance is used as a benchmark. Tables 2 and 3 present the values of our evaluation metrics for different continuous-control tasks. We set $\alpha = 0.9$ for VaR_α and $CVaR_\alpha$ and estimate all metrics with $N = 50$ sampled trajectories (as followed by [Ho and Ermon, 2016]). The following are some interesting observations that we make:

- RAIL obtains superior performance than GAIL at both tail risk measures – $VaR_{0.9}$ and $CVaR_{0.9}$, without increasing sample complexity. This shows that RAIL is a superior choice than GAIL for imitation learning in risk-sensitive applications.
- The applicability of RAIL is not limited to environments in which the distribution of trajectory-cost is heavy-tailed for GAIL. [Rockafellar and Uryasev, 2000] showed that if the distribution of the risk variable Z be normal, $CVaR_\alpha(Z) = \mu_Z + a(\alpha)\sigma_Z$, where $a(\alpha)$ is a constant for a given α , μ_Z and σ_Z are the mean and standard deviation of Z . Thus, in the absence of a heavy tail, minimization of $CVaR_\alpha$ of the trajectory cost aids in learning better policies by contributing to the minimization of the mean and standard deviation of trajectory cost. The results on Reacher-v1 corroborate our claims. Although the histogram does not show a heavy tail (Figure 3 in Appendix B), the mean converges fine (Figure 2) and tail risk scores are improved (Table 2) which indicates the distribution of trajectory-costs is more condensed around the mean than GAIL. Thus we can use RAIL instead of GAIL, no matter whether the distribution of trajectory costs is heavy-tailed for GAIL or not.
- Figure 2 shows the variation of mean trajectory cost over training iterations for GAIL and RAIL. We observe that RAIL converges almost as fast as GAIL at all the continuous-control tasks in discussion, and at times, even faster.
- The success of RAIL in learning a viable policy for Humanoid-v1 suggests that RAIL is scalable to large environments. Scalability is one of the salient features of GAIL. RAIL preserves the scalability of GAIL while showing lower tail risk.

RAIL agents show lesser tail risk than GAIL agents after training has been completed. However it still requires the agent to act in the real world and sample trajectories (line 3 in Algorithm 1) during training. One way to rule out environmental interaction during training is to make the agent act in a simulator while learning from the expert’s real-world demonstrations. The setting changes to that of third person imitation learning [Stadie et al., 2017]. The RAIL formulation can be easily ported to this framework but we do not evaluate that in this paper.

7 Conclusion

This paper presents the RAIL algorithm which incorporates $CVaR$ optimization within the original GAIL algorithm to minimize tail risk and thus improve the reliability of learned policies. We report significant improvement over GAIL at a number of evaluation metrics on five continuous-control tasks. Thus the proposed algorithm is a viable step in the direction of learning low-risk policies by imitation learning in complex environments, especially in risk-sensitive applications like robotic surgery and autonomous driving. We plan to test RAIL on fielded robotic applications in the future.

Acknowledgments

The authors would like to thank Apoorv Vyas of Intel Labs and Sapana Chaudhary of IIT Madras for helpful discussions. Anirban Santara’s travel was supported by Google India under the Google India PhD Fellowship Award.

References

- Pieter Abbeel and Andrew Y Ng. Apprenticeship learning via inverse reinforcement learning. In *Proceedings of the twenty-first international conference on Machine learning*, page 1. ACM, 2004.
- Pieter Abbeel and Andrew Y Ng. Inverse reinforcement learning. In *Encyclopedia of machine learning*, pages 554–558. Springer, 2011.
- Pieter Abbeel, Adam Coates, Morgan Quigley, and Andrew Y Ng. An application of reinforcement learning to aerobatic helicopter flight. In *Advances in neural information processing systems*, pages 1–8, 2007.
- Brenna D. Argall, Sonia Chernova, Manuela Veloso, and Brett Browning. A survey of robot learning from demonstration. *Robotics and Autonomous Systems*, 57(5):469 – 483, 2009. ISSN 0921-8890. doi: <http://dx.doi.org/10.1016/j.robot.2008.10.024>. URL <http://www.sciencedirect.com/science/article/pii/S0921889008001772>.
- Christopher G Atkeson and Stefan Schaal. Robot learning from demonstration. In *ICML*, volume 97, pages 12–20, 1997.
- Mariusz Bojarski, Davide Del Testa, Daniel Dworakowski, Bernhard Firner, Beat Flepp, Praseem Goyal, Lawrence D Jackel, Mathew Monfort, Urs Muller, Jiakai Zhang, et al. End to end learning for self-driving cars. *arXiv preprint arXiv:1604.07316*, 2016.
- Mariusz Bojarski, Philip Yeres, Anna Choromanska, Krzysztof Choromanski, Bernhard Firner, Lawrence Jackel, and Urs Muller. Explaining how a deep neural network trained with end-to-end learning steers a car. *arXiv preprint arXiv:1704.07911*, 2017.
- Vivek S Borkar. Q-learning for risk-sensitive control. *Mathematics of operations research*, 27(2): 294–311, 2002.
- Greg Brockman, Vicki Cheung, Ludwig Pettersson, Jonas Schneider, John Schulman, Jie Tang, and Wojciech Zaremba. Openai gym. *arXiv preprint arXiv:1606.01540*, 2016.
- Yinlam Chow and Mohammad Ghavamzadeh. Algorithms for cvar optimization in mdps. In *Advances in neural information processing systems*, pages 3509–3517, 2014.
- Nivine Dalleh. *Why is CVaR superior to VaR?(c2009)*. PhD thesis, 2011.
- Hal Daumé, John Langford, and Daniel Marcu. Search-based structured prediction. *Machine learning*, 75(3):297–325, 2009.
- Jimmy Ba Diederik Kingma. Adam: A method for stochastic optimization. *arXiv:1310.5107 [cs.CV]*, 2015.
- Chelsea Finn, Sergey Levine, and Pieter Abbeel. Guided cost learning: Deep inverse optimal control via policy optimization. In *International Conference on Machine Learning*, pages 49–58, 2016.
- Javier Garcia and Fernando Fernández. A comprehensive survey on safe reinforcement learning. *Journal of Machine Learning Research*, 16(1):1437–1480, 2015.
- Paul W Glimcher and Ernst Fehr. *Neuroeconomics: Decision making and the brain*. Academic Press, 2013.
- Ian Goodfellow, Jean Pouget-Abadie, Mehdi Mirza, Bing Xu, David Warde-Farley, Sherjil Ozair, Aaron Courville, and Yoshua Bengio. Generative adversarial nets. In *Advances in neural information processing systems*, pages 2672–2680, 2014.
- Simon Haykin. *Neural Networks: A Comprehensive Foundation*. Prentice Hall PTR, Upper Saddle River, NJ, USA, 2nd edition, 1998. ISBN 0132733501.
- Matthias Heger. Consideration of risk in reinforcement learning. In *Proceedings of the Eleventh International Conference on Machine Learning*, pages 105–111, 1994.
- Jonathan Ho and Stefano Ermon. Generative adversarial imitation learning. In *Advances in Neural Information Processing Systems*, pages 4565–4573, 2016.

- Ronald A Howard and James E Matheson. Risk-sensitive markov decision processes. *Management science*, 18(7):356–369, 1972.
- Ming Hsu, Meghana Bhatt, Ralph Adolphs, Daniel Tranel, and Colin F Camerer. Neural systems responding to degrees of uncertainty in human decision-making. *Science*, 310(5754):1680–1683, 2005.
- Investopedia. Definition of tail risk. <http://www.investopedia.com/terms/t/tailrisk.asp>, 2017. Accessed: 2017-09-11.
- Sham Kakade and John Langford. Approximately optimal approximate reinforcement learning. In *ICML*, volume 2, pages 267–274, 2002.
- Sergey Levine and Vladlen Koltun. Continuous inverse optimal control with locally optimal examples. *arXiv preprint arXiv:1206.4617*, 2012.
- Timothy P. Lillicrap, Jonathan J. Hunt, Alexander Pritzel, Nicolas Heess, Tom Erez, Yuval Tassa, David Silver, and Daan Wierstra. Continuous control with deep reinforcement learning. *CoRR*, abs/1509.02971, 2015. URL <http://arxiv.org/abs/1509.02971>.
- Anirudha Majumdar, Sumeet Singh, Ajay Mandlekar, and Marco Pavone. Risk-sensitive inverse reinforcement learning via coherent risk models. 2017.
- Oliver Mihatsch and Ralph Neuneier. Risk-sensitive reinforcement learning. *Machine learning*, 49(2-3):267–290, 2002.
- Volodymyr Mnih, Koray Kavukcuoglu, David Silver, Andrei A Rusu, Joel Veness, Marc G Bellemare, Alex Graves, Martin Riedmiller, Andreas K Fidjeland, Georg Ostrovski, et al. Human-level control through deep reinforcement learning. *Nature*, 518(7540):529–533, 2015.
- Arne J Nagengast, Daniel A Braun, and Daniel M Wolpert. Risk-sensitive optimal feedback control accounts for sensorimotor behavior under uncertainty. *PLoS computational biology*, 6(7):e1000857, 2010.
- Andrew Y Ng, Stuart J Russell, et al. Algorithms for inverse reinforcement learning. In *Icml*, pages 663–670, 2000.
- Yael Niv, Jeffrey A Edlund, Peter Dayan, and John P O’Doherty. Neural prediction errors reveal a risk-sensitive reinforcement-learning process in the human brain. *Journal of Neuroscience*, 32(2): 551–562, 2012.
- OpenAI-GAIL. Imitation learning github repository. <https://github.com/openai/imitation.git>, 2017. Accessed: 2017-06-27.
- Dean A Pomerleau. Alvin: An autonomous land vehicle in a neural network. In *Advances in neural information processing systems*, pages 305–313, 1989.
- Aravind Rajeswaran, Sarvjeet Ghotra, Sergey Levine, and Balaraman Ravindran. Epopt: Learning robust neural network policies using model ensembles. *5th International Conference on Learning Representations*, 2016.
- R Tyrrell Rockafellar and Stanislav Uryasev. Optimization of conditional value-at-risk. *Journal of risk*, 2:21–42, 2000.
- Stéphane Ross and Drew Bagnell. Efficient reductions for imitation learning. In *Proceedings of the thirteenth international conference on artificial intelligence and statistics*, pages 661–668, 2010.
- Stephane Ross and J Andrew Bagnell. Reinforcement and imitation learning via interactive no-regret learning. *arXiv preprint arXiv:1406.5979*, 2014.
- Stéphane Ross, Geoffrey J Gordon, and Drew Bagnell. A reduction of imitation learning and structured prediction to no-regret online learning. In *International Conference on Artificial Intelligence and Statistics*, pages 627–635, 2011.

- Stuart Russell. Learning agents for uncertain environments. In *Proceedings of the eleventh annual conference on Computational learning theory*, pages 101–103. ACM, 1998.
- Andrzej Ruszczyński. Risk-averse dynamic programming for markov decision processes. *Mathematical programming*, 125(2):235–261, 2010.
- Stefan Schaal. Learning from demonstration. In *Advances in neural information processing systems*, pages 1040–1046, 1997.
- John Schulman, Sergey Levine, Philipp Moritz, Michael I. Jordan, and Pieter Abbeel. Trust region policy optimization. *CoRR*, abs/1502.05477, 2015. URL <http://arxiv.org/abs/1502.05477>.
- Shai Shalev-Shwartz, Shaked Shammah, and Amnon Shashua. Safe, multi-agent, reinforcement learning for autonomous driving. *arXiv preprint arXiv:1610.03295*, 2016.
- Shai Shalev-Shwartz, Shaked Shammah, and Amnon Shashua. On a formal model of safe and scalable self-driving cars. *arXiv preprint arXiv:1708.06374*, 2017.
- Yun Shen, Michael J Tobia, Tobias Sommer, and Klaus Obermayer. Risk-sensitive reinforcement learning. *Neural computation*, 26(7):1298–1328, 2014.
- David Silver, Aja Huang, Chris J Maddison, Arthur Guez, Laurent Sifre, George Van Den Driessche, Julian Schrittwieser, Ioannis Antonoglou, Veda Panneershelvam, Marc Lanctot, et al. Mastering the game of go with deep neural networks and tree search. *Nature*, 529(7587):484–489, 2016.
- Bradly C Stadie, Pieter Abbeel, and Ilya Sutskever. Third-person imitation learning. *arXiv preprint arXiv:1703.01703*, 2017.
- R.S. Sutton and A.G. Barto. *Reinforcement Learning: An Introduction*. A Bradford book. Bradford Book, 1998. ISBN 9780262193986. URL <https://books.google.co.in/books?id=CAFR6IBF4xYC>.
- Emanuel Todorov, Tom Erez, and Yuval Tassa. Mujoco: A physics engine for model-based control. In *Intelligent Robots and Systems (IROS), 2012 IEEE/RSJ International Conference on*, pages 5026–5033. IEEE, 2012.
- Brian D Ziebart. *Modeling Purposeful Adaptive Behavior with the Principle of Maximum Causal Entropy*. PhD thesis, Carnegie Mellon University, 2010.
- Brian D Ziebart, Andrew L Maas, J Andrew Bagnell, and Anind K Dey. Maximum entropy inverse reinforcement learning. In *AAAI*, volume 8, pages 1433–1438. Chicago, IL, USA, 2008.

Appendix

A Calculation of Gradients of the CVaR term

In this section we derive expressions of gradients of the CVaR term in equation 9 w.r.t. π , \mathcal{D} , and ν . Let us denote $H_\alpha(D^\pi(\xi|c(\mathcal{D})), \nu)$ by \mathcal{L}_{CVaR} . Our derivations are inspired by those shown by Chow and Ghavamzadeh [2014].

- **Gradient of \mathcal{L}_{CVaR} w.r.t. \mathcal{D} :**

$$\begin{aligned}\nabla_{\mathcal{D}} \mathcal{L}_{CVaR} &= \nabla_{\mathcal{D}} \left[\nu + \frac{1}{1-\alpha} \mathbb{E}_{\xi \sim \pi} [(D^\pi(\xi|c(\mathcal{D})) - \nu)^+] \right] \\ &= \frac{1}{1-\alpha} \mathbb{E}_{\xi \sim \pi} [\nabla_{\mathcal{D}} D^\pi(\xi|c(\mathcal{D})) \mathbf{1}(D^\pi(\xi|c(\mathcal{D})) \geq \nu)]\end{aligned}\quad (\text{A.1})$$

where $\mathbf{1}(\cdot)$ denotes the *indicator function*. Now,

$$\nabla_{\mathcal{D}} D^\pi(\xi|c(\mathcal{D})) = \nabla_c D^\pi(\xi|c(\mathcal{D})) \nabla_{\mathcal{D}} c(\mathcal{D}) \quad (\text{A.2})$$

$$\begin{aligned}\nabla_c D^\pi(\xi|c(\mathcal{D})) &= \nabla_c \sum_{t=0}^{L_\xi-1} \gamma^t c(s_t, a_t) \\ &= \sum_{t=0}^{L_\xi-1} \gamma^t \\ &= \frac{1 - \gamma^{L_\xi}}{1 - \gamma}\end{aligned}\quad (\text{A.3})$$

Substituting equation A.3 in A.2 and then A.2 in A.1, we have the following:

$$\nabla_{\mathcal{D}} \mathcal{L}_{CVaR} = \frac{1}{1-\alpha} \mathbb{E}_{\xi \sim \pi} \left[\frac{1 - \gamma^{L_\xi}}{1 - \gamma} \mathbf{1}(D^\pi(\xi|c(\mathcal{D})) \geq \nu) \nabla_{\mathcal{D}} c(\mathcal{D}) \right] \quad (\text{A.4})$$

- **Gradient of \mathcal{L}_{CVaR} w.r.t. π :**

$$\begin{aligned}\nabla_{\pi} \mathcal{L}_{CVaR} &= \nabla_{\pi} H_\alpha(D^\pi(\xi|c(\mathcal{D})), \nu) \\ &= \nabla_{\pi} \left[\nu + \frac{1}{1-\alpha} \mathbb{E}_{\xi \sim \pi} [(D^\pi(\xi|c(\mathcal{D})) - \nu)^+] \right] \\ &= \frac{1}{1-\alpha} \nabla_{\pi} \mathbb{E}_{\xi \sim \pi} [(D^\pi(\xi|c(\mathcal{D})) - \nu)^+] \\ &= \frac{1}{1-\alpha} \mathbb{E}_{\xi \sim \pi} [(\nabla_{\pi} \log P(\xi|\pi))(D^\pi(\xi|c(\mathcal{D})) - \nu)^+]\end{aligned}\quad (\text{A.5})$$

- **Gradient of \mathcal{L}_{CVaR} w.r.t. ν :**

$$\begin{aligned}\nabla_{\nu} \mathcal{L}_{CVaR} &= \nabla_{\nu} \left[\nu + \frac{1}{1-\alpha} \mathbb{E}_{\xi \sim \pi} [(D^\pi(\xi|c(\mathcal{D})) - \nu)^+] \right] \\ &= 1 + \frac{1}{1-\alpha} \mathbb{E}_{\xi \sim \pi} [\nabla_{\nu} (D^\pi(\xi|c(\mathcal{D})) - \nu)^+] \\ &= 1 - \frac{1}{1-\alpha} \mathbb{E}_{\xi \sim \pi} [\mathbf{1}(D^\pi(\xi|c(\mathcal{D})) \geq \nu)]\end{aligned}\quad (\text{A.6})$$

B Additional figures

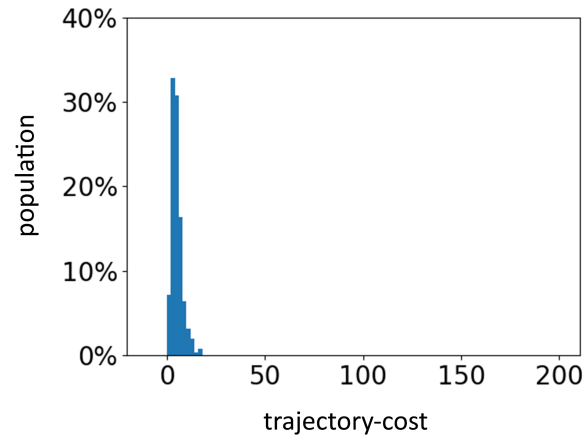


Figure 3: Histogram of costs of 250 trajectories generated by a GAIL-learned policy for Reacher-v1. The distribution shows no heavy tail. From Table 2 and Figure 2, we observe that RAIL performs as well as GAIL even in cases where the distribution of trajectory costs is not heavy-tailed.